NORTHWEST AFRICA 8326: THE MOST STRONGLY SHOCKED HOWARDITE-EUCRITE-DIOGENITE METEORITE. L. Zhang[1], A. C. Zhang[1], X. W. Liu[1], J. N. Chen, and Y. Y. Wen[2]. [1]School of Earth Sciences and Engineering, Nanjing University, Nanjing 210023, China, [2]Institute of Geochemistry, Chinese Academy of Sciences, Guiyang 550081, China, E-mail: LangZhang@smail.nju.edu.cn

Introduction: Impact plays an important role in the evolution of planetary bodies [1–2]. The impact conditions can be constrained based on shock-induced high-pressure (HP) minerals [3]. Many HP minerals indicating strong shock metamorphism (e.g., > 20 GPa) have been observed in ordinary chondrites and Martian meteorites, but rarely reported in howardite-eucrite-diogenite (HED) meteorites. A few HP minerals were recently described in HED meteorites, suggesting moderate shock metamorphism [4–13]. In this study, we report the shock-induced HP mineral assemblages within and adjacent to shock melt veins in the noritic eucrite Northwest Africa (NWA) 8326 and suggest that NWA 8326 be the most strongly shocked HED meteorite up to date.

Methods: A Zeiss Supra 55 field-emission SEM was used for petrographic observations. The JEOL 8230/8530F EPMA instruments were used for determining chemical composition of minerals. Structural characterization of minerals was carried out using Laser Raman spectroscopy and electron back-scatter diffraction.

Five FIB sections were observed using the F20 TEM instrument at Nanjing University. Selected area electron diffraction under TEM mode, HAADF imaging, EDS analyses, and elemental mapping under STEM mode were performed for structural and chemical characterization of mineral phases.

Results: NWA 8326 consists mainly of enstatite (~75 vol%), plagioclase (~19 vol%), and augite (~5 vol%). Augite occurs as either exsolution lamellae at the margin of enstatite or an intergranular phase. Plagioclase has partially transformed into maskelynite. Accessory minerals include silica, chromite, merrillite, ilmenite, zircon, baddeleyite, troilite, and Fe-Ni metal. NWA 8326 is considered as a noritic eucrite in this study, based on the mineral assemblage and the relatively high Ti concentrations in pyroxene and chromite that are more consistent with eucrite rather than diogenite.

A few shock melt veins are present in NWA 8326 and their widths vary from a few μm to ~150 μm. They have various chemical compositions and contain different HP mineral assemblages.

Most of the shock melt veins are composed of fine-grained clinopyroxene and garnet, with clinopyroxene being dominated at the edge and garnet at the center. The clinopyroxene grains are cation-deficient (3.8–3.9 apfu based on 6 oxygen atoms), indicating high concentrations of cation vacancy. Garnet exhibits three various occurrences: cryptocrystalline garnet, dendritic garnet, and granular garnet from the edge to the center of the shock melt veins (Figs. 1a and 1b). They all are super silicic and show a decrease of Si concentration from the edge to the center of the veins (3.8 apfu to 3.2 apfu Si based on 12 oxygen atoms; Fig. 2).

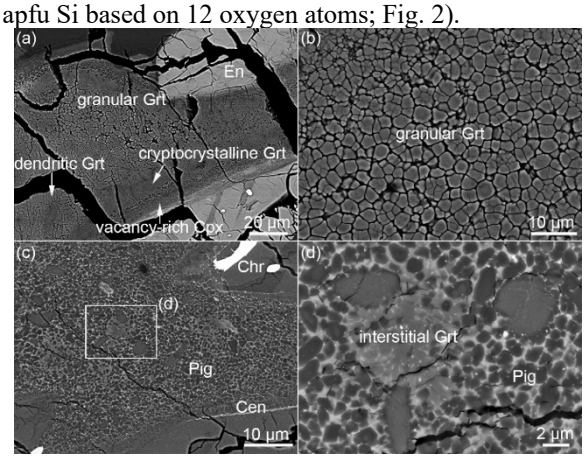

Fig. 1: BSE images of the high-pressure minerals in the shock melt veins. Grt=Garnet, En=Enstatite, Cpx=Clinopyroxene, Pig=Pigeonite, Cen=Clinoenstatite, and Chr=Chromite.

A few shock melt veins contain clinoenstatite, pigeonite, and garnet from the edge to the center (Figs. 1c and 1d). In these veins, the garnet grains appear as an irregular interstitial phase in BSE images (Fig. 1d), but TEM observations show that they are granular in shape. These garnet grains are highly majoritic and contain ~3.7 apfu Si and ~0.4 apfu Al (Fig. 2).

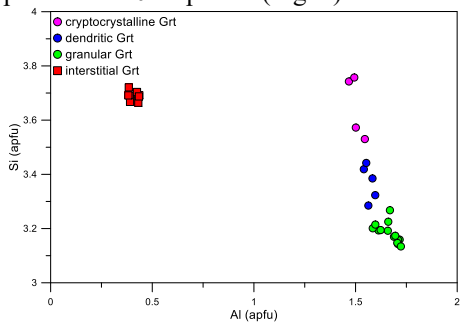

Fig. 2: Chemical composition of super-silicic garnet , calculations are based on 12 oxygen atoms

In a few maskelynite regions adjacent to shock melt veins, fine-grained tissintite aggregates are present along the interface with surrounding minerals based on their Raman spectra.

High-pressure minerals stishovite, xieite, tuite, and reidite were also observed adjacent to the shock melt veins or in the host rock (Fig. 3). They were identified based on their petrographic occurrences and Raman spectra. Stishovite is present as a fibrous aggregate at the boundary between a large silica grain and pyroxene (Fig. 3a). Xieite appears as bright lamellae in the chromite grains adjacent to shock melt veins and forms a zone of ~5 μm in width (Fig. 3b). Tuite was identified in a large merrillite grain adjacent to a shock melt vein (Fig. 3c). Reidite appears as brighter lamellae in zircon (Fig. 3d). Interestingly, no shock melt veins were observed with a distance of 3 mm from reidite in the section plane.

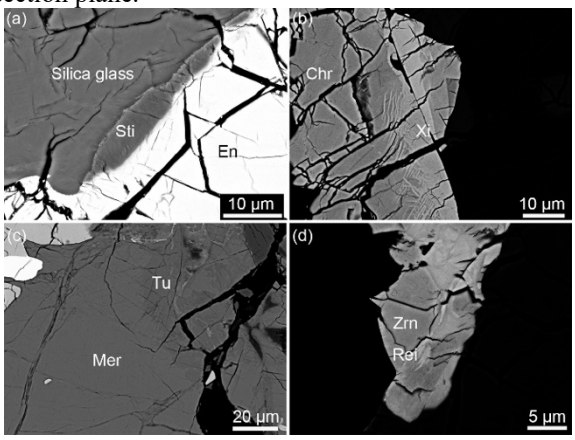

Fig. 3: BSE images of high-pressure minerals adjacent to the shock melt veins or in the host rock. Sti=Stishovite, Xi=Xieite, Mer=Merrillite, Tu=Tuite, Zrn=Zircon, and Rei=Reidite.

Discussion and Conclusion: High-pressure minerals in shock melt veins generally crystallize from HP melts during pressure release [14]. Therefore, they can be used to constrain the lower limit of crystallization pressure of shock melt veins. In NWA 8326, vacancy-rich clinopyroxene and clinoenstatite are both present at the edge of shock melt veins. However, they have too wide stability fields (vacancy-rich clinopyroxene (from < 2 GPa to > 20 GPa, [15]); Clinoenstatite (> 6 GPa, [16]) to properly constrain the crystallization pressure. Instead, the crystallization pressure can be estimated based on the Si and Al concentrations of super-silicic garnet [17]. The compositions of cryptocrystalline garnet (3.8 apfu Si) and interstitial majoritic garnet (3.7 apfu Si) indicate that the crystallization pressure of the shock melt veins may be high up to at least 18 GPa.

Stishovite, xieite, tuite, and reidite are the high-pressure phase of silica, chromite, merrillite, and zircon respectively. Essentially identical compositions imply that they have formed through solid-state transformation under high pressures. Based on static HP experimental results, quartz transforms into stishovite at pressure above 7.5 GPa [18], merrillite transforms into tuite at pressure above 14 GPa [19], chromite and zircon transform into xieite and reidite at pressure above 20 GPa, respectively [20–21]. Therefore, the presence of the HP minerals formed through solid-state transformation indicates that NWA 8326 should have experienced a shock pressure of at least 20 GPa.

In previous investigations, shock pressures of a few eucrites have been constrained by different methods. For instance, the shock pressure of Béréba (8–13 GPa, [4]), NWA 8003 (> 10 GPa), NWA 2650 (> 8 GPa), and Padvarninkai (2–13 GPa) were estimated based on static HP experiments [4, 5, 10–13]. On the contrast, the shock pressure for NWA 10658 (> 24 GPa) and Padvarninkai (22–27 GPa) were constrained based on dynamic HP experiments [5–6]. If based on the stability field of HP minerals, the shock pressures would be < 8 GPa and 2–13 GPa for NWA 10658 and Padvarninkai, respectively. Comparing with the HP minerals in these shocked eucrites, the HP minerals in NWA 8326 record the highest crystallization pressure of shock melt veins in these shocked eucrites. Therefore, it may be reasonable to state that NWA 8326 is the most strongly shocked HED meteorite up to date.

References: [1] Collins G. S. et al. (2012) *Elements, 8,* 25–30. [2] Gillet P. and El Goresy A. (2013) *Annu. Rev. Earth Plant. Sci, 41,* 257–285. [3] Tomioka N. and Miyahara M. (2017) *Meteorit. and Planet. Sci, 52,* 2017–2039. [4] Miyahara M. et al. (2014) *Proc. Natl. Acad. Sci, 111,* 10939–10942. [5] Miyahara M. et al. (2021) *Meteorit. and Planet. Sci, 56,* 1443–1458. [6] Fudge C. et al. (2017) *LPSC XLVIII,* Abstract #2525. [7] Fudge C. et al. (2018) *LPSC XLIX,* Abstract #2417. [9] Fudge C. et al. (2019) *LPSC L,* Abstract #2077. [8] Fudge C. and Sharp T. G. (2020) *LPSC LI,* Abstract #1783. [10] Pang R. L. et al. (2016) *Sci. Rep, 6,* 26063. [11] Pang R. L. et al. (2018) *Am. Mineral, 103,* 1502–1511. [12] Pang R. L. et al. (2019) *Geochemistry, 79,* 125541. [13] Chen D. L. et al. (2019) *Meteorit. and Planet. Sci, 44,* 359–374. [14] Fritz J. et al. (2017) *Meteorit. and Planet. Sci, 52,* 1216–1232.[15] Liu L. (1980) *EPSL, 47,* 398–402. [16] Shinmei T. et al. (1999) *Am. Mineral, 84,* 1588–1594. [17] Glass B. P. and Liu S. B. (2001) *Geology, 4,* 371–373. [18] Zhang J. et al. (1995) *Phys. Chem. Minerals, 23,* 1–10. [19] Xie X. D. et al. (2002) *Geochim. Cosmochim. Acta, 66,* 2439–2444. [20] Chen M. et al. (2003) *Proc. Natl. Acad. Sci, 100,* 14651–14654. [21] Aoki I. and Takahashi E. (2004) *Phys. Earth Plant. Inter, 143–144,* 129–143.

Acknowledgements: This work was financially supported by research grants from NSFC (42025302, 41973061, 41673068), CAS (XDB41000000), and CNSA (grant D020204).